Scanning Force Microscopy Study of Etch Pits Formed during Dissolution of a Barite (001) Surface in CDTA and EDTA Solutions

Kang-Shi Wang,[†] Roland Resch,[‡] Kai Dunn,[†] Patrick Shuler,[§] Yongchun Tang,[§] Bruce E. Koel,[‡] and Teh Fu Yen*,[†]

Department of Civil and Environmental Engineering, University of Southern California, Los Angeles, California 90089, Department of Chemistry, University of Southern California, Los Angeles, California 90089, and Chevron Petroleum Technology Company, La Habra, California 90631

Received March 10, 1999. In Final Form: June 30, 1999

Dissolution of the barite (001) surface in aqueous solutions of 0.18 M CDTA (*trans*-1,2-cyclohexylenediaminetetraacetic acid) and 0.18 M EDTA (ethylenediaminetetraacetic acid) at pH 12 was investigated using ex situ scanning force microscopy. In both solutions, triangular and trapezoidal etch pits developed on the (001) surface and became deeper and longer with increasing dissolution time. The orientation of the etch pits in CDTA and EDTA solutions was elongated along the crystallographic *b* axis. Furthermore, dissolution of the (001) surface in a layer-by-layer fashion was observed. This resulted in the formation of "alternating" etch pits with heights of one half-unit cell (about 3.6 Å), with the orientations of any two consecutive etch pits pointing oppositely to each other. In CDTA, etch pits within the half-unit cell were frequently bounded along the ⟨120⟩ and ⟨010⟩ directions. However, in EDTA, etch pits within the half-unit cell were bounded along the ⟨110⟩ and ⟨010⟩ directions. The dissolution behavior of barite in these two solutions is different based on the observed differences in the etch pits geometries as an assay for specific interactions between the crystal surface and organic molecules. Thus, we suggest that CDTA molecules bind to one Ba^{2+} cation along the ⟨120⟩ and/or ⟨010⟩ directions and EDTA molecules bind along the ⟨110⟩ directions to two Ba^{2+} cations exposed on the (001) surface.

Introduction

Barite ($BaSO_4$) is one of the most common[1] and obstinate scales[2] found in offshore oil and gas production systems. Due to its relatively low solubility ($K_{sp} = 10^{-9.99}$ at 25 °C) in water,[3] barite scale deposits easily from brine (typically 1−20% dissolved salt) once its solubility limit has been exceeded. Barite precipitates suspended in the water cause problems such as plugging pore spaces in the oil-producing formation and adherent scale on surfaces such as pipe walls, valves, and pumps. Both effects are highly undesirable and result in restricted fluid flow and equipment damage. Effective scale control is a primary objective of any efficient handling operation.

The use of chelating agents as dissolvers for the removal of mineral scales has been recently studied.[4,5] DTPA (diethylenetriaminepentaacetic acid) is believed to be the most effective scale dissolver[6] and has proven its ability under field conditions.[7] In this study, we selected two alternative chelating agents, *trans*-1,2-cyclohexylenediaminetetraacetic acid (CDTA) and ethylenediaminetetraacetic acid (EDTA), to investigate interfacial interactions between these agents and the barite (001) surface. The kinetics of the dissolution of bulk barite scale in the presence of these polyaminocarboxylic compounds have demonstrated that these scale dissolvers significantly increase the dissolution rate of the barite scale.[8] An understanding of fundamental dissolution processes should aid attempts to develop new cost-effective scale-dissolving products.

The ligands $CDTA^{4-}$ and $EDTA^{4-}$ are shown schematically in Figure 1. Their coordination with Ba^{2+} cations in aqueous solution at 25 °C have formation constants of log $K_{ML} = 8.69$ and log $K_{ML} = 7.86$, respectively.[9] These values indicate that both tetranegative anions are capable of complexing Ba^{2+} cations in a 1:1 (ligand:metal) ratio in aqueous solutions at high pH.[10] Binding to the metal center occurs with four carboxylate oxygen atoms and two nitrogen atoms. Consequently, the ligands have a strong tendency to bond with metal ions exposed on the surface of the scale. The strong bonding between the metal cations and the ligands weakens the cation−anion interaction, and eventually the ligands remove the metal cations into the solution. This results in scale dissolution.

Scanning force microscopy (SFM) has proven to be a powerful tool for studying surface topography. Time-

* To whom correspondence should be addressed: Department of Civil and Environmental Engineering, 3620 South Vermont Avenue, KAP 224A , University of Southern California, Los Angeles, CA 90089-2531; Tel, (213) 740-0586; fax, (213) 744-1426; e-mail, tfyen@mizar.usc.edu.

[†] Department of Civil and Environmental Engineering, University of Southern California.

[‡] Department of Chemistry, University of Southern California.

[§] Chevron Petroleum Technology Company.

(1) Cowan, J. C.; Weintritt, D. J. *Water Formed Scale Deposits*; Gulf Publishing Co.: Houston, 1976.

(2) Vetter, O. J. *J. Pet. Technol.* **1975**, Dec., 1515.

(3) Högfeldt, E. *Stability Constants of Metal-Ion Complexes. Part A: Inorganic Ligands*; Pergamon Press: Oxford, 1982.

(4) Morris, R. L.; Paul, J. M. U. S. Patent No. 4,980,077, 1990.

(5) Rhudy, J. S. SPE 25161 1993, presented at the SPE International Symposium on Oilfield Chemistry, New Orleans, LA.

(6) Putnis, A.; Putnis, C. V.; Paul, J. M. SPE 29094 1995, presented at the SPE International Symposium on Oilfield Chemistry, San Antonio, TX.

(7) Lejon, K.; Vikane, O. SPE 31126 1996, presented at the SPE Formation Damage Control Symposium, Lafayette, LA.

(8) Dunn, K. Ph.D. Thesis, University of Southern California, Los Angeles, 1999.

(9) Smith, R. M.; Martell, A. E. *Critical Stability Constants*; Plenum Press: New York, 1974; Vol. 1.

(10) Martell, A. E.; Hancock, R. D. *Metal Complexes in Aqueous Solutions*; Plenum Press: New York, 1996.

10.1021/la990285x CCC: $19.00
Published on Web 10/19/1999

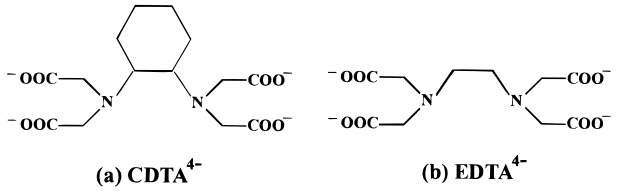

Figure 1. Molecular structures of polyaminoacetate scale dissolvers: (a) $CDTA^{4-}$; (b) $EDTA^{4-}$.

resolved observations of processes on/at surfaces can provide considerable insights into reaction mechanisms on an atomic level between active molecules and a flat, cleaved surface. It is most desirable to perform in situ experiments under liquids in order to study growth and dissolution processes of crystals in real time without contaminants or water layers introduced by ambient exposures.[11−14] However, artifacts are often introduced in the case of in situ observations by contact mode SFM in reactive solutions where surface is undergoing rapid dissolution.[15−18] This is because the SFM tip accelerates the dissolution processes due to the tip/surface interaction, which can result in surface modification (e.g., deeper and larger etch pits). On the other hand, when the rate of dissolution occurs too slowly such as when the concentration of active molecules is too small, the influence of water on the dissolution processes cannot be neglected. Furthermore, by definition, time-resolved in situ experiments should be performed under flow-through conditions.[19] This introduces, in most cases, a thermal drift resulting in poorer resolution and artifacts.

In situ investigations utilizing dynamic SFM and contact mode SFM under liquids, as performed in our lab, showed that artifacts are easily introduced in studies of barite dissolution with chelating agents at concentrations higher than 0.06 M. These artifacts (e.g., a rounded shape at the pit edges and/or the artificial creation or leveling of steps) could make it difficult to accurately analyze the morphology of the etch pit. For these reasons and the fact that the general dissolution behavior of terraces on a (001) barite surface is homogeneous, we believe that ex situ dynamic SFM is a good probe for this study. In these techniques,[20] the cantilever oscillates at (or near) its resonant frequency with the tip at a few nanometers above the sample surface or the tip in intermittent contact with the sample. Changes in the oscillation amplitude reveal the topography of the sample. Since the tip is either in noncontact or in intermittent contact with the sample surface, damage to the surface and/or surface modification caused by lateral shear forces[21] can be minimized.

The aim of this paper is, therefore, to investigate the dissolution behavior of the barite (001) surface under aqueous solutions of EDTA and CDTA by ex situ dynamic SFM. This gives new insights to the interactions of the chelating agents with the barite (001) surface. In this study we do not provide measurements of the dissolution kinetics of barite (001) surface. Our observations show the morphology of etch pits on the barite (001) surface after dissolution. It is important to understand how the morphology of dissolution layers with molecular heights is related to the structure of the crystal surface. We have found that the various morphologies of the etch pits produced depend not only on the surface crystallographic structure but also on the nature of the chelating agent.

Experimental Section

Materials. Natural barite crystals were used from the Barrick Meikle mine in Nevada. The bulk composition of the samples was $(Ba_{0.91},Sr_{0.09})SO_4$, as analyzed by XRAL Laboratories, Canada. The presence of strontium (Sr) in barite crystals has little effect on the morphology of barite.[22] The clear and colorless crystal was freshly cleaved in ambient air with a sharp knife blade placed on a (210) face along the *b* axis and parallel to (001) face.

CDTA Solution. CDTA (*trans*-1,2-cyclohexylenediaminetetraacetic acid), 6.56 g (ICN Biochemicals Co.), was added to 90 mL of deionized water and NaOH was then added. The pH was adjusted to about 12 to ensure the full deprotonation of CDTA. CDTA solutions (0.18 M) of 100 mL were made up with deionized water.

EDTA Solution. EDTA (ethylenediaminetetraacetic acid), 5.26 g (Baker Chemicals Co.), was added to 90 mL of deionized water, and NaOH was then added. The pH was adjusted to about 12 to ensure the full deprotonation of EDTA. EDTA solutions (0.18 M) of 100 mL were made up with deionized water.

Sample Preparation. Barite crystals were freshly cleaved, and a (001) surface was observed in air by dynamic SFM prior to any treatments. The sample was dipped into an unstirred etching solution for a given time at room temperature (20 °C) and subsequently rinsed with deionized water. Rinsing of the sample with only deionized water does not remove adsorbed CDTA and EDTA clusters (this has been confirmed by studies using Auger electron spectroscopy). Deposition of these clusters strongly interfered with dynamic SFM observations. Therefore, we had to use 0.5 M HCl for rinse of the crystal prior to imaging. However, this HCl rinse had an effect on the barite (001) surface, and this can be minimized by a short (∼10 s) rinse procedure. The effect of the 0.5 M HCl rinse for 10 s on the barite (001) surface is shown in Figure 2. Triangular etch pits (less than one unit cell in height) and deep etch pits (1−2.5 unit cells in height) were induced by the HCl rinse on flat terraces. In comparison to using only a water rinse, HCl formed more etch pits on the barite (001) surface. Cleaning the surface is an important preparation for making high-quality ex situ observations of surface microtopography.

SFM Instrumentation. A Park Scientific Instruments (PSI) Autoprobe CP scanning probe microscope (SPM) was operated in dynamic mode. All cantilevers used in this study were commercially available, triangularly shaped Si cantilevers obtained from PSI with a resonance frequency of about 250 kHz and a spring constant of about 13 N/m. The cantilevers were driven with a setpoint amplitude of about 8 nm and a free amplitude of 9−10 nm. All imaging was performed in air at room temperature.

(11) Bosbach, D.; Rammensee, W. *Geochim. Cosmochim. Acta* **1994**, *58*, 843.
(12) Hall, C.; Cullen, D. C. *AIChE J.* **1996**, *42*, 232.
(13) Higgins, S. R.; Jordan, G.; Eggleston, C. M. *Langmuir* **1998**, *14*, 4967.
(14) Shindo, H.; Shitagami, K.; Kondo, S.; Seo, A. *J. Cryst. Growth* **1999**, *198/199*, 253.
(15) Delawski, E.; Parkinson, B. A. *J. Am. Chem. Soc.* **1992**, *114*, 1661.
(16) Maurice, P. A.; Hochella, M. F., Jr.; Parks, G. A.; Sposito, G.; Schwertmann, U. *Clays Clay Miner.* **1995**, *43*, 29.
(17) Resch, R.; Friedbacher, G.; Grasserbauer, M. *Fresenius' J. Anal. Chem.* **1997**, *358*, 352.
(18) Schmitz, I.; Schreiner, M.; Friedbacher, G.; Grasserbauer, M. *Anal. Chem.* **1997**, *69*, 1012.
(19) Dove, P. M.; Chermak, J. In CMS Workshop Lectures, *Scanning Probe Microscopy of Clay Minerals*; Nagy, K., Blum, A. E., Eds.; The Clay Minerals Society: Boulder, CO, 1994; Vol. 7, p 139.
(20) Chi, L. F. *Appl. Phys. A* **1999**, *68*, 203.
(21) Overney, R. M.; Takano, H.; Fujihira, M.; Meyer, E.; Güntherodt, H.-J. *Thin Solid Films* **1994**, *240*, 105.
(22) Redfern, S. E.; Parker, S. C. *J. Chem. Soc., Faraday Trans.* **1998**, *94* (14), 1947.

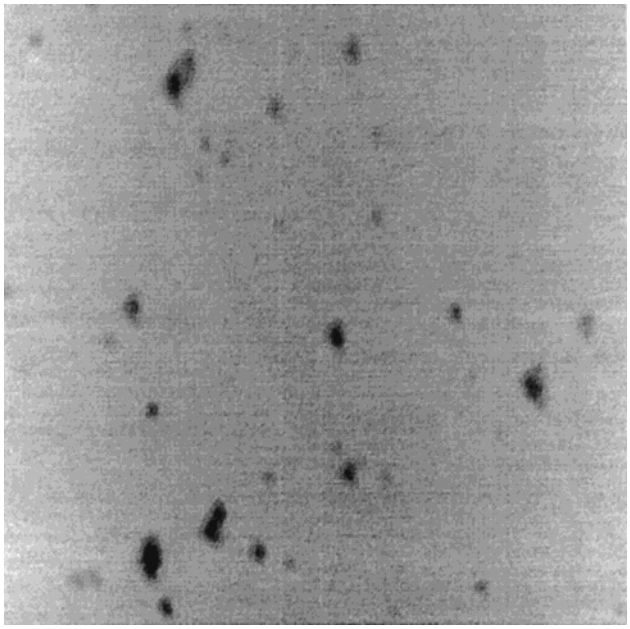

Figure 2. Dynamic SFM image of a barite (001) surface after dissolution in 0.5 M HCl for 10 s. Image size is 1 μm × 1 μm. Depth scale from black to white is 2.5 nm.

The scan rate was 1.5 Hz, and a resolution of 512 pixels × 512 pixels per image was selected.

Results and Discussion

(001) Surface Structure. Barite ($BaSO_4$) has an orthorhombic structure (space group P_{nma}, with lattice constants a = 8.884 Å, b = 5.457 Å, c = 7.157 Å, and Z = 4)[23] and shows a characteristic perfect (001) cleavage plane. Computer models of the ideally terminated and unreconstructed (001) surface were made with the commercial Cerius2 simulation package as shown in Figure 3. Each unit cell has two $BaSO_4$ layers parallel to (001), and each layer is related by a 2_1 screw axis parallel to the c axis.[24] Figure 3a shows the topmost monolayer of the (001) surface seen down along the c axis. This layer contains Ba−Ba periodic bond chains (PBCs)[25] along [100], [010], [110], and [120] directions with repeat periods of 8.88, 5.46, 10.43, and 14.07 Å, respectively. These crystallographic orientations represent the stronger bond within one $BaSO_4$ layer predicted from PBC theory. The arrows in Figure 3b illustrate the influence of the 2_1 screw axis that is parallel to the c axis. The direction between adjacent barium cations and sulfate anions changes between layers. Relaxation of the outermost surface has been calculated to be slight under vacuum,[26] and reconstruction of (001) surface does not occur in aqueous solution at room temperature.[27]

Dynamic SFM images of the freshly cleaved barite (001) surface that we obtained were consistent with morphologies reported by others.[28] Typically, cleavage generated a few steps with one and/or multiples of one unit-cell height (i.e., c = 7.16 Å). The orientation of these steps was not related to the energetically stable crystallographic directions. In general, these steplines indicate the direction and velocity of crack propagation.[29]

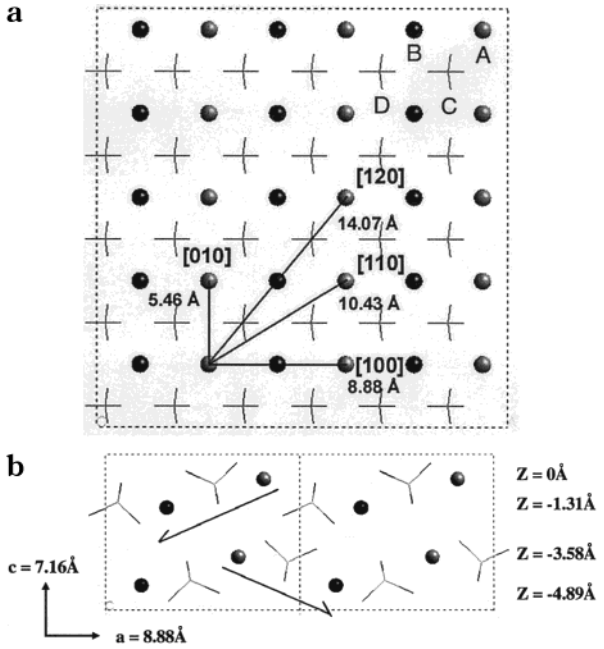

Figure 3. Computer models of the $BaSO_4$ (001) surface. (a) (top view) The topmost monolayer of (001) surface is seen down along the c axis direction. The topmost Ba^{2+} cations at z = 0 (marked as A) are represented by lighter gray balls. The Ba^{2+} cations at z = −1.31 Å (marked as B) are represented by darker balls. The tetrahedral "sticks" (marked as C) represent SO_4^{2-} anions that are below the topmost Ba^{2+} cations. While those (marked as D) represent SO_4^{2-} anions that are above the lower Ba^{2+} cations. The four PBC vectors of the (002) slice are shown as along the [100], [010], [110], and [120] directions. (b) (side view) The structure of the (001) surface is seen along the b axis direction. The first row of Ba^{2+} cations is defined at height z = 0, and then other deeper Ba^{2+} cations occur at z = −1.31, −3.58, and −4.89 Å. The two arrows indicate different important directions for Ba^{2+}−SO_4^{2-} bonding in consecutive layers, which are related to a 2_1 screw axis parallel to the c axis. The Ba^{2+} cations are represented as gray and black balls. There are two orientations of SO_4^{2-} anions, which are represented as tetrahedral stick figures (sulfur, gray; oxygen, black).

Dissolution of the Barite (001) Surface in CDTA Solution. Barite is very insoluble in water at room temperature. In our previous NC-AFM observations of barite dissolution in deionized water, the images showed only a few shallow, triangular etch pits on the (001) surface after immersion for up to 1 h.[30] However, the addition of alkaline solutions of chelating agents such as CDTA and EDTA remarkably increased the dissolution rate of barite.[8]

Figure 4 shows a representative set of SFM images of dissolution features on the flat (001) surface that was treated with 0.18 M CDTA solutions for 1, 3, 10, and 40 min. Although these images were obtained from different areas of the surface of the barite crystal, we observed a uniform dissolution behavior of terraces at the (001) surface for a given dissolution time. These images are representative of features that exist over the entire surface. Etch pits produced by CDTA molecules elongated along the b axis and grew deeper along the c axis as the exposure time was increased.

After 1 min of dissolution, shallow triangular etch pits (one-half of a unit cell in height) denoted as "1", and deep etch pits (1−3 unit cells in height) denoted as "2" were

(23) Miyake, M.; Minato, I.; Morikawa, H.; Iwai, S.-I. *Am. Mineral.* **1978**, *63*, 506.
(24) Pina, C. M.; Becker, U.; Risthaus, P.; Bosbach, D.; Putnis, A. *Nature* **1998**, *395*, 483.
(25) Hartman, P.; Strom, C. S. *J. Cryst. Growth* **1989**, *97*, 502.
(26) Allan, N. L.; Rohl, A. L.; Gay, D. H.; Catlow, R. A.; Davey, R. J.; Mackrodt, W. C. *Faraday Discuss.* **1993**, *95*, 273.
(27) Bosbach, D.; Hall, C.; Putnis, A. *Chem. Geol.* **1998**, *151*, 143.
(28) Putnis, A.; Junya-Rosso, J. L.; Hochella, M. F., Jr. *Geochim. Cosmochim. Acta* **1995**, *59*, 4623.
(29) DE Wainer, L. S.; Bassett, G. A. *Philos. Mag. A* **1978**, *38*, 707.
(30) Wang, K.-S.; Resch, R.; Dunn, K.; Shuler, P.; Tang, Y.; Koel, B. E.; Yen, T. F. *Colloids Surf., A*, in press.

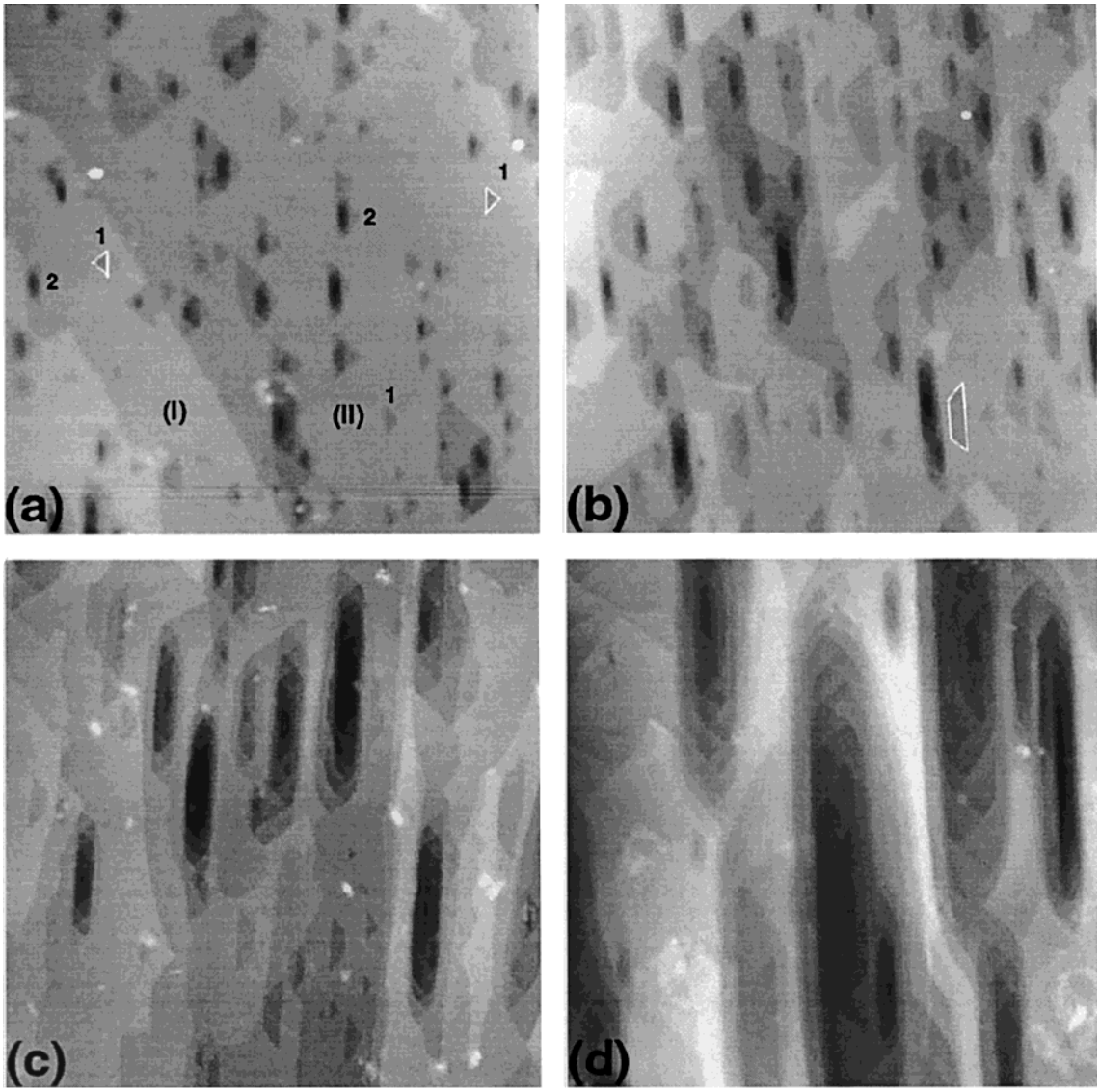

Figure 4. Dynamic SFM images of a barite (001) surface after dissolution in 0.18 M CDTA for (a) 1, (b) 3, (c) 10, and (d) 40 min. Image size is 1.5 μm × 1.5 μm. Depth scale from black to white is (a) 3, (b) 5, (c) 7, and (d) 10 nm. The image in (a) shows triangular etch pits that are one-half of a unit cell deep denoted as "1". Two opposite orientations of etch pits are related by the 2_1 screw axis parallel to the *c* axis. Deep etch pits (1−3 unit cells in depth) are denoted as "2". The image in (b) shows one of the trapezoidal etch pits (marked with a white outline) that has a depth:width:length ratio of 1:175:525.

observed on the terraces as shown in Figure 4a. The depth of the three cleavage steps is about 3.6 Å (one-half of a unit cell). A few of the small (less than 45 nm in width, 75 nm in length), shallow triangular etch pits may appear due to the HCl rinse. In layer I, all triangular etch pits have the same orientation, but the etch pits in layer II, which is one-half of a unit cell height lower, was oriented oppositely to those in layer I. The two opposite orientations of etch pits are related by the 2_1 screw axis parallel to the *c* axis. Although Figure 4a does not show a [010] step, our observations (not shown) revealed that these steps remained smooth and straight indicating that no dissolution took place along [010] steps in a 1-min dissolution. Steps with different orientations, not along [010], became ragged in a 1-min dissolution implying that they were easily dissolved.

As the dissolution time increased, the shallow triangular pits subsequently coalesced with neighboring pits and/or developed from an individual pit into trapezoidal etch pits (one-half of a unit cell in height) as shown in Figure 4b taken after 3 min. Measurements on one of the shallow, trapezoidal etch pits (marked with a white outline) gave a depth:width:length ratio of 1:175:525. Most of these pits possessed an internal angle of 42 ± 4°, indicating that the pits are bounded along the ⟨010⟩ and ⟨120⟩ directions at one end. This angle agrees favorably with the value of 39° expected from the crystal geometry. A few of the pits have an internal angle of 54 ± 4° at the end indicating that the pits are bounded along the ⟨010⟩ and ⟨110⟩ directions. This is close to the value of 58° expected from the crystal geometry. The trapezoidal etch pits grew deeper along the *c* axis and more elongated along the [010] direction with increasing dissolution time. The dissolution of the trapezoidal etch pits is highly anisotropic. The steps parallel to [120] advanced faster than those parallel to [010]. This is because the advancing rate of steps that contain a low kink density is controlled by the stronger bond directions within the surface.[31]

The etch pits that are deeper than one unit cell are composed of several alternating trapezoidal pits. All etch pits in the same monolayer are oriented in the same

(31) Sunagawa, I. *Morphology of Crystals: Part A*; Terra Scientific Publishing Co.: Tokyo, 1987; Chapter 5.

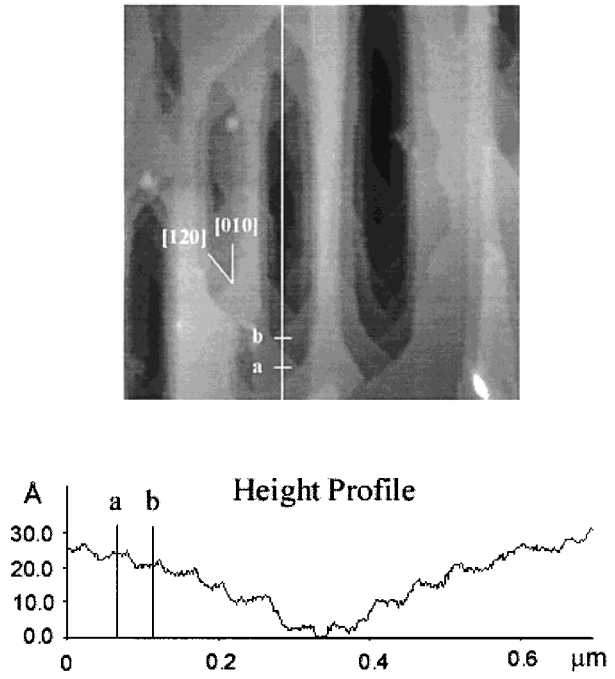

Figure 5. (top) Dynamic SFM image of a barite (001) surface following dissolution in 0.18 M CDTA for 10 min. (bottom) A line profile taken across the pit along the *b* axis. The morphology of etch pits was defined by monolayer steps parallel to the [010] and [120] directions. Flat terraces at the bottoms of the etch pits were observed. The height difference between the two terraces denoted as a and b is 3.64 Å. Image size is 0.7 μm × 0.7 μm. Depth scale from black to white is 6 nm.

direction, and all etch pits in the underlying layer are oriented in the opposite direction. Again, this phenomenon is due to the 2_1 screw axis parallel to the *c* axis and a layer-by-layer dissolution process. A line profile measurement of one of these etch pits in Figure 4c is shown at higher magnification in Figure 5. This reveals terraces with one-half and one unit cell steps. The formation of such deep etch pits is similar with the observations in barite dissolution in EDTA by Bosbach et al.[27] and in DTPA by Putnis et al.[28] These pits expanded along the [010] and [001] directions with a length:depth ratio of between 100:1 and 200:1 for increasing dissolution time. These pits dominate the images as shown in panels c and d of Figure 4. The geometry of these deep pits is termed "trapezohedral" because of the superimposed effect of two opposite orientations of alternating terraces of these etch pits. The greatest depth of these deep etch pits was 6−11 unit cells as shown in panels c and d of Figure 4, respectively. Growth of the etch pits occurred laterally faster than vertically, and so the depth of the etch pits increased only slowly with time because of the layer-by-layer dissolution mechanism.

Mechanism of CDTA for Controlling Etch Pit Morphology. On the basis of the observed angles for the morphology of etch pits, we suggest that donor groups in CDTA may be preferentially adsorbed along the ⟨120⟩ and/or ⟨010⟩ directions. The PBCs along the ⟨120⟩ and ⟨110⟩ directions are formed by the bond with chain repeating period of 14.07 and 10.43 Å, respectively. CDTA contains a rigid hydrophobic cyclohexyl ring, and the nitrogen donors in $CDTA^{4-}$ are held in the trans form with the acetate groups constrained to be closer together than those in $EDTA^{4-}$.[10] Therefore, the acetate donor groups in $CDTA^{4-}$ may not be able to coordinate to two partially exposed Ba^{2+} cations along the ⟨120⟩ or ⟨110⟩ directions and may orient into a position to coordinate to only one partially exposed Ba^{2+} cation. Removal of one such cation forms the edge of an etch pit bounded along the ⟨120⟩ directions (the most prevalent pits in our studies). The face along the ⟨120⟩ directions is the lowest energy surface in the barite crystal.[26,32] According to theoretical calculations of EDTA binding to the barite (001) surface by Blanco et al.,[32] a high-energy barrier may limit movement of the EDTA molecule along the [100] direction and the binding site is located along the channels running parallel to the [010] direction. We expect that a similar situation is valid for CDTA. Our observations of the morphology of trapezoidal etch pits can be consistent within the framework provided by these theoretical calculations. The orientations of the edges of a trapezoidal etch pit (one-half of a unit cell in height) other than ⟨120⟩ (or ⟨110⟩) and ⟨010⟩ directions were never observed.

Dissolution of the Barite (001) Surface in EDTA Solution. Dissolution experiments in EDTA solution show types of etch pits and dissolution processes that are similar to those in CDTA solution. Figure 6a shows a dynamic SFM image obtained after 1 min of dissolution in EDTA solution. Many triangular etch pits (one-half of a unit cell in depth) and few deep etch pits (more than one unit cell in depth) were randomly distributed on the flat terraces. Again, a few of the small (less than 45 nm in width, 75 nm in length), shallow triangular etch pits may be produced because of the HCl rinse. Figure 6b displays the topography after 3 min of dissolution. Features in this image have step heights of *c*/2. The triangular pits have opposite orientations on adjacent terraces. This indicates that the pits produced are controlled by the 2_1 screw axis parallel to the *c* axis as we noted earlier. The deep etch pits (1−3 unit cells in depth) were more abundant after 3 min than those observed after 1 min of dissolution.

Dissolution in EDTA solution for 5 min produced trapezoidal etch pits (one-half of a unit cell in depth) as shown in Figure 7. These deep pits showed an alternating "step-edge" orientation for each alternating half-unit cell. Thus, dissolution proceeds in a layer-by-layer process and is controlled by the 2_1 screw axis parallel to the *c* axis. Line profile measurements of these characteristic etch pits support this further. One of the deep etch pits as shown in Figure 7 is made of four alternating trapezoidal etch pits. Each pit is one-half of a unit cell in height. The internal angles of the two ends of these pits were measured to be 54 ± 4°. This agrees well with the internal angle of 58° that can be calculated for an etch pit edge bounded along the ⟨010⟩ and ⟨110⟩ directions. Similar trapezoidal etch pits have been observed on barite (001) surfaces in the presence of other dissolvers, i.e., DTPA[28,30] and CDTA, which have similar amino acetate functional groups.

Mechanism of EDTA for Controlling Etch Pit Morphology. According to in situ observations by Bosbach et al.,[27] steps parallel to the [110] direction retreat faster than do [010] steps. In panels c and d of Figures 6, we observed etch pits elongated along the *b* axis which is consistent with this result. However, in contrast to Bosbach et al., we see that the morphology of deep etch pits is due to a superposition of two orientations of alternating trapezoidal etch pits. In our studies with EDTA solutions, we did not observe any shallow etch pits with a [010]−[110] morphology that develop into deep etch pits with a [010]−[100] morphology. This is possibly because there is an energy barrier that limits movement of the EDTA molecule along the *a* axis.[32]

The trapezoidal morphology of EDTA etch pits is different from those produced by CDTA. This indicates

(32) Blanco, M.; Tang, Y.; Shuler, P.; Goddard, W. A., III *Mol. Eng.* **1997**, *7*, 491.

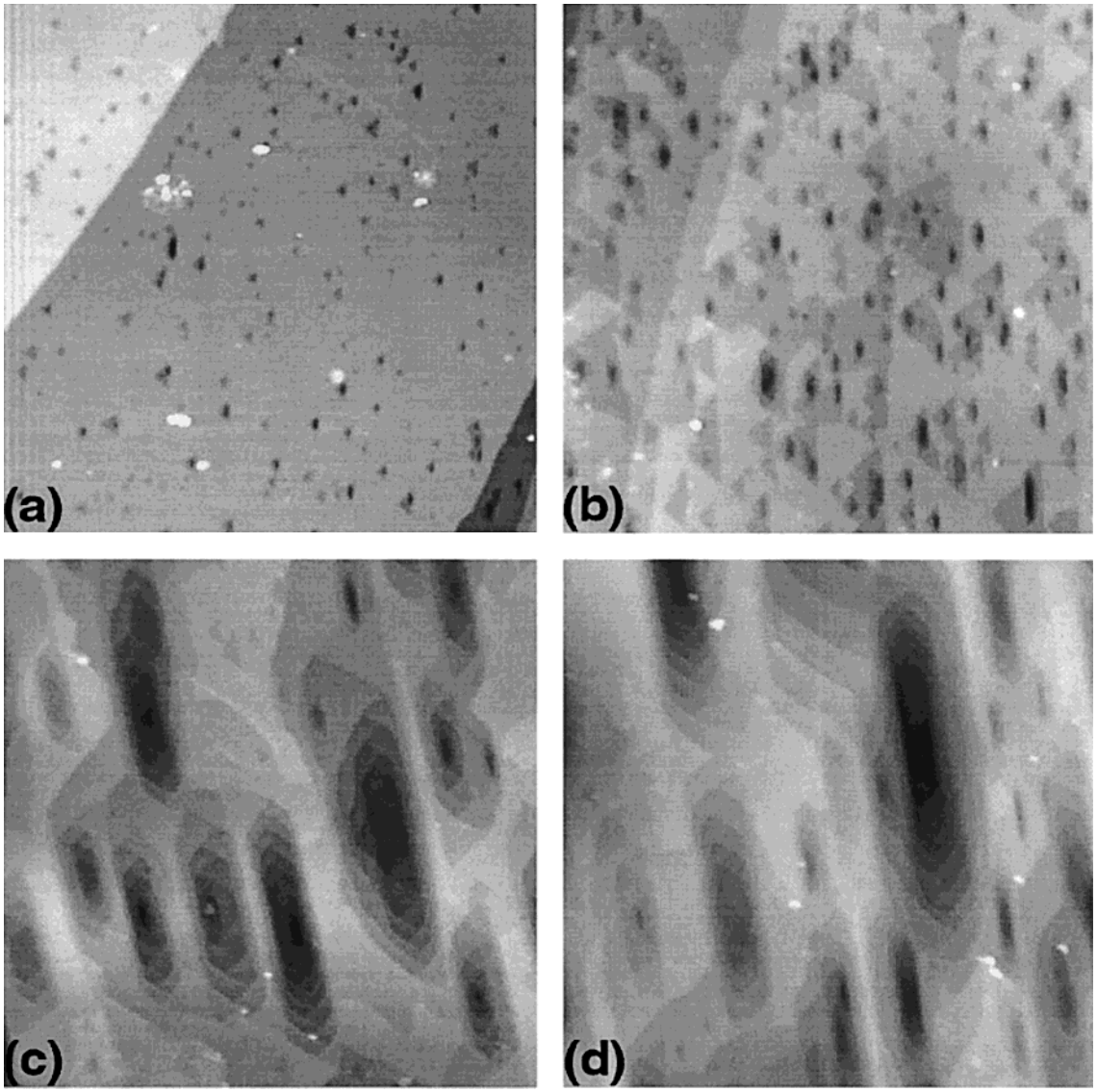

Figure 6. Dynamic SFM images of a barite (001) surface after dissolution in 0.18 M EDTA for (a) 1, (b) 3, (c) 10, and (d) 40 min. Image size is 1.5 μm × 1.5 μm. Depth scale from black to white is (a) 3, (b) 4, (c) 8, and (d) 12 nm.

that the binding geometries of the adsorbed ligand and dissolution processes may be different for these two dissolvers. According to Blanco et al.[32] in their study using activated complex theory of barite scale control processes, $EDTA^{4-}$ molecules maximize the interaction with the (001) surface by orienting the molecular axis along the ⟨110⟩ direction. The PBC along the ⟨110⟩ directions is formed with a chain repeating period of 10.43 Å. EDTA molecules can coordinate to such two partially exposed Ba^{2+} cations along the ⟨110⟩ directions when the acetate donor groups are fully extended. Removal of these cations results in an edge of an etch pit bounded along the ⟨110⟩ and ⟨010⟩ directions. Large energy barriers (15 kcal/mol) prevent the side movement of $EDTA^{4-}$ molecules along the *a* axis.[32] This explains why we observed elongated etch pits always along the *b* axis.

Formation of Etch Pits in CDTA and EDTA Solutions. Similar shallow triangular etch pits and deep etch pits were found on the (001) surface during early stages of barite dissolution in etching solutions (i.e., CDTA, EDTA, DTPA,[30] and HCl[33]). The step orientations of triangular pits were aligned with the more stable directions such as ⟨120⟩, ⟨010⟩, and/or ⟨110⟩ . The smaller, shallow etch pits observed on the atomically flat terraces at the beginning are due to two-dimensional nucleation of new pits. This occurs in the absence of crystal defects. Each deep etch pit containing several alternating trapezoidal pits has a nearly flat bottom. This suggests that the etch pits are produced by two-dimensional nucleation or that the pits develop at defects such as point defects.[34] The larger pits, after a longer time, continue to grow beyond a critical radius. The edges of the pits can appear as steps or line defects on the surface, which are favorable sites for dissolution.[35] It should be noted that dissolution spirals from dislocations do not appear in our observations. This indicates that the pits do not originate at a screw dislocation intersecting the surface. The shape of the etch pit formed from the coalescence of smaller pits is not simply determined by the CDTA or EDTA molecules in the dissolving solution but also is affected by the physical arrangement and spatial distribution of defect outcrops.

Ligand-Promoted Dissolution Studies. The chelating agents (DTPA,[30] CDTA, and EDTA) that we have studied all contain the same type of functional groups, yet

(33) Wang, K.-S.; Resch, R.; Dunn, K.; Shuler, P.; Tang, Y.; Koel, B. E.; Yen, T. F. *J. Colloids Interface Sci.*, in press.
(34) Onuma, K.; Ito, A.; Tabe, I.; Tateishi, T. *J. Phys. Chem. B* **1997**, *101*, 8534.
(35) Blum, A. E.; Yund, R. A.; Lasaga, A. C. *Geochim. Cosmochim. Acta* **1990**, *54*, 283.

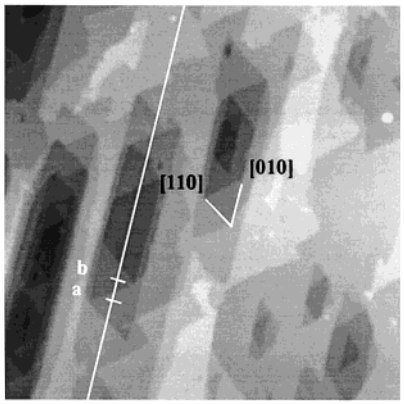

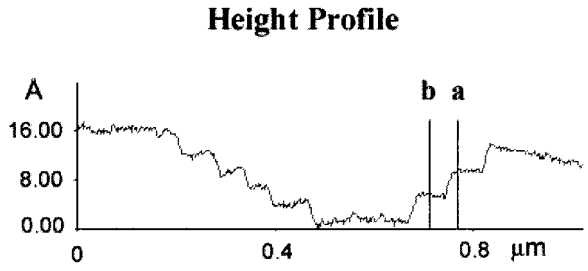

Figure 7. (top) Dynamic SFM image of a barite (001) surface following dissolution in 0.18 M EDTA for 5 min. (bottom) A line profile taken across a pit along the *b* axis. The morphology of etch pits was defined by monolayer steps parallel to the [010] and ⟨110⟩ directions. Flat terraces at the bottoms of the etch pits were observed. The height difference between the two terraces denoted as a and b is 3.61 Å. Image size is 1 μm × 1 μm. Depth scale from black to white is 4 nm.

produce different etch pit morphologies. This suggests that the ability of a compound to enhance crystal dissolution depends not only on its ability to form surface complexes but also on the size and geometry of these complexes relative to a specific crystal surface.

As a final point, scale dissolution is a heterogeneous reaction. One has to consider the role of the solid−solution interface in the dissolution mechanism. However, a detailed understanding of the mechanisms of complexation reactions and also of the factors that determine the complex stability on the surface has not yet been achieved. Further molecular imaging and molecular modeling studies are required to probe the energetics and mechanisms of the adsorption and detachment processes of organic dissolvers on the crystal surfaces.

Conclusions

Ex situ dynamic SFM observations of dissolution of a barite ($BaSO_4$) crystal reveal that etch pits characteristic of enhanced dissolution could be observed by adding chemical dissolvers such as CDTA and EDTA. Solutions containing these dissolvers develop larger and deeper etch pits than pure water solution and cause an increase in the overall dissolution rate. Shallow triangular and trapezoidal etch pits that are one-half of a unit cell in depth were formed in the early dissolution stages in all solutions. Due to the importance in the barite structure of the 2_1 screw axis parallel to the *c* axis, trapezoidal etch pits were produced with opposite orientations in consecutive layers. Deep etch pits are formed by a layer-by-layer etching process. In CDTA solutions, the orientation of the monolayer step edges is along the ⟨010⟩ and ⟨120⟩ directions. However, in EDTA solutions, the orientation of the monolayer step edges is along the ⟨010⟩ and ⟨110⟩ directions. We rationalize the shapes and orientations of etch pit developed on this particular crystal face by considering the molecular level details of the reaction mechanisms of CDTA and EDTA. We propose that the active sites of CDTA molecules coordinate to one Ba^{2+} cation exposed on the (001) surface. In contrast, the active sites of EDTA molecules bond simultaneously to two Ba^{2+} cations exposed on the (001) surface along the ⟨110⟩ directions.

Acknowledgment. Financial support of T. F. Yen from the Chevron Petroleum Technology Company and of B. E. Koel from the Z. A. Kaprielian Technology Innovation Fund are gratefully acknowledged. We thank the Laboratory for Molecular Robotics at USC for use of the SFM facility and donation of barite crystals from Barrick Meikle mine. The authors thank Dr. M. Blanco, Dr. Y. H. Jang, and Professor W. A. Goddard III in the Materials and Process Simulation Center at CIT for their contributions of computer models. We also thank Professor C. M. Eggleston and Professor P. E. Russell for helpful comments during review.

LA990285X